Angewandte Chemie
Eine Zeitschrift der Gesellschaft Deutscher Chemiker

Supporting Information

Single Particle Nanoelectrochemistry Reveals the Catalytic Oxygen Evolution Reaction Activity of Co_3O_4 Nanocubes

*Thomas Quast[+], Swapnil Varhade[+], Sascha Saddeler, Yen-Ting Chen, Corina Andronescu, Stephan Schulz, and Wolfgang Schuhmann**

anie_202109201_sm_miscellaneous_information.pdf

Supporting Information

Table of Contents

SUPPORTING INFORMATION

Section 1: Experimental procedures

Chemicals and materials

Ethanol (absolute ≥99.8% VWR Chemicals), toluene (Sigma-Aldrich), potassium hydroxide (Fisher Chemical), cobalt (II) acetylacetonate [$Co(acac)_2$; 99%], hexamethylendiamine (HMDA; 98%), oleylamine (OLA; ≥98%),N-Boc-ethylenediamine (>98%), and $LiClO_4$, were purchased from Sigma-Aldrich. [(Os (2, 2'-bipyridine)$_2$(N, N'-dimethyl-2, 2´-biimidazole)] $(PF_6)_3$ was synthesised as reported earlier.[1] Cobalt(II) nitrate hexahydrate (99 %) and sodium hydroxide (98 %) were purchased from abcr and used as received.
Single barrel quartz capillaries (0.9 mm inner diameter, 1.2 mm outer diameter, 10 cm length) with filaments (WAR-QTF-120-90) and single barrel quartz capillaries (0.9 mm inner diameter, 1.2 mm outer diameter, 7.5 cm length) were purchased from Sutter Instruments.

Synthesis and Charactersiaton

X-ray diffraction (XRD) patterns of the sample were recorded at ambient temperature with a Bruker D8 Advance powder diffractometer in Bragg-Brentano geometry with CuK_α radiation (l = 1.5418 Å, 40 kV, and 40 mA) in the range from 5 to 90°. The size and morphology of the nanoparticles were determined using a JEOL 2200FS transmission electron microscope. Energy dispersive X-ray spectroscopy (EDX) studies were performed using a JEOL JSM6510 scanning electron microscope equipped with an energy dispersive X-ray detector (BrukerQuantax400). The obtained spectra were quantified by using the software Esprit 1.9 (Bruker).

SECCM

The quartz capillaries were cleaned with isopropanol and then pulled using a P-2000 laser puller (Sutter Instruments) with the one-line program with parameters: Heat 730-780, Filament 3, Velocity 30, Delay 130, Pull 80-100. Scanning electron micrographs were recorded using a Quanta 3D ESEM (FEI) at 20 kV or 30 kV in the high vacuum mode.
The SECCM set-up comprises a positioning system, a current amplifier, and a voltage amplifier connected to an FPGA card. The three stepper motors (Owis) with a LStep PCIe (Lang) controller as well as x,y,z-piezocube (Physik Instrumente) with analogue piezo amplifier (Physik Instrumente) were used for coarse and fine movement of the sample relative to the SECCM tip, respectively (Figure S9). The working principle of the SECCM was reported previously.[1,2] Current amplifier (DLPCA-200, Femto) and voltage amplifier (DLPVA-100-B, Femto) are used to monitor the current responses during single-barrel capillary experiments. The current amplifier exhibited a signal-to-noise level of less than 1 pA. The whole set-up is placed inside a Faraday cage and mounted on an active vibration damping table (RS 2000, Newport).

Particle at the tip

Quartz capillaries were pulled using a P-2000 laser puller (Sutter Instruments) using the following pulling parameters: HEAT=740, FILAMENT=4, VELOCITY=45, DELAY=130, and PULL=100. Scanning electron micrographs were recorded using a Quanta 3D ESEM (FEI) at 30 kV in the high vacuum mode. Electrostatic charging of the carbon nanoelectrodes was prevented by inserting a copper wire from the back end of the capillary, which is essential for an effective FIB milling process. Focused ion beam (FIB) milling of the as-prepared CNEs was performed using the Quanta 3D ESEM, which is equipped with a Ga-FIB source. High-resolution transmission electron microscopy (HR-TEM) was performed using a JEOL microscope (JEM-2800) equipped with a Schottky-type emission source working at 200 kV, Gatan OneView camera (4kx4k, 25FPS) to obtain images with a resolution of 0.09 nm. Energy dispersive spectroscopy (EDS) elemental mapping was performed using double silicon drift detectors (SDD), with a solid angle of 0.98 steradians with a detection area of 100 mm^2. Electrochemical measurements were performed inside a Faraday cage in precleaned 1.0 M or 0.1 M KOH, which was placed inside another Faraday cage, using a ModuLab potentiostat from Solartron Analytical in a two-electrode configuration using a homemade double junction Ag/AgCl/3M KCl as both reference and counter electrode.

Section 2: Synthesis and characterization of Co_3O_4 nanocubes

A solution of 1.60 g (40 mmol) NaOH in 5 mL of water was added at ambient temperature to a stirred solution of 11.64 g (40 mmol) of $Co(NO_3)_2$ x 6 H_2O in 25 mL H_2O, yielding a pink precipitate. The suspension was transferred into a 50 mL stainless-steel autoclave with Teflon inset and heated in an electric furnace to 180 °C for 5 h. The resulting crystalline product was centrifugated (3000 rpm, 10 min), washed two times with water and one time with acetone and dried at ambient temperature.

The hydrothermal synthesis yielded spinel-type Co_3O_4 nanoparticles (Fig. S1a) without any traces of crystalline secondary phases such as hydroxides, as was proven by Rietveld refinement (Fig. S1b). The synthesized spinel-type Co_3O_4 nanocubes did not show any changes in their crystall structure after a heating step at 200 °C as shown by XRD and Rietveld refinement. The lattice parameter (8.088 Å) is in good agreement with values previously reported for Co_3O_4 (8.072 Å).[3] The average particle size was determined to 207 nm by using the Scherrer equation. The Rietveld refinement shows a texture effect identified by a stronger (400) reflex compared to the reference pattern. This texture effect is in accordance with the formation of cubic-shaped nanoparticles.

SUPPORTING INFORMATION

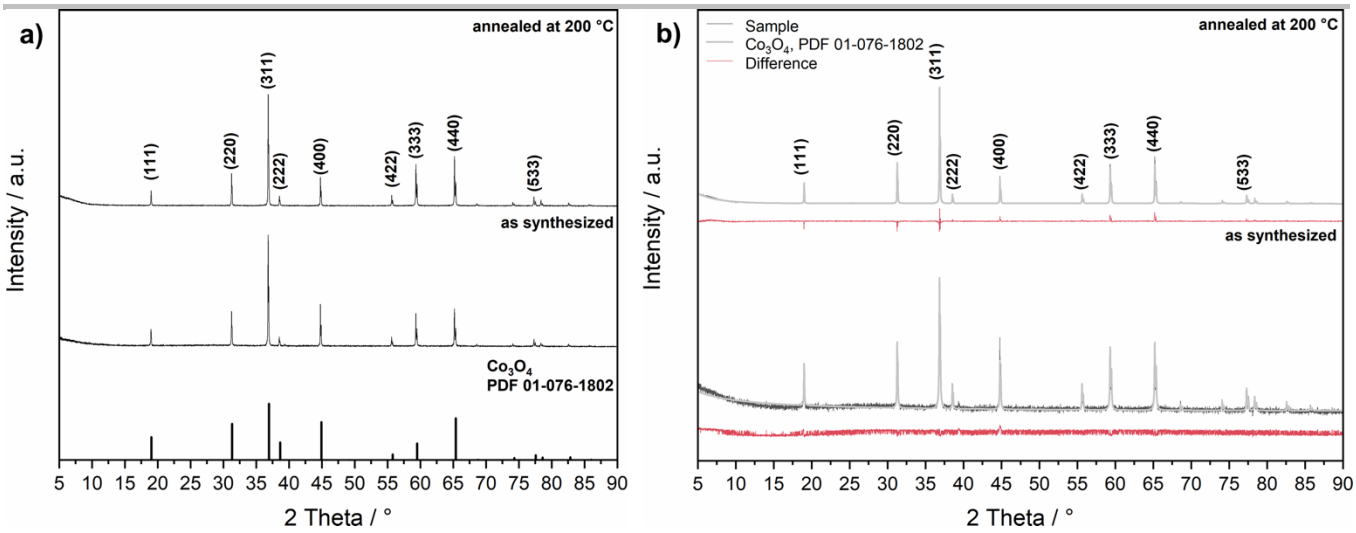

Figure S1. a) XRD pattern and b) Rietveld refinement of cubic Co_3O_4 nanoparticles as synthesized and after the annealing step at 200 °C.

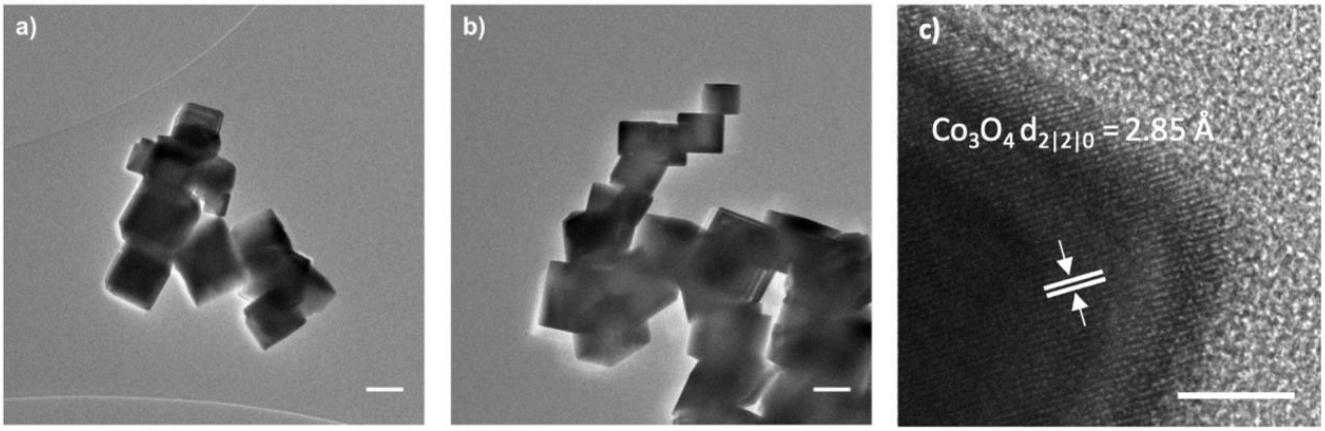

Figure S2. TEM images of cubic Co_3O_4 nanoparticles. Scale bars: 200 nm (a, b) and 10 nm (c).

In Figure S2 TEM micrographs of the synthesized Co_3O_4 cubes are shown. The size distribution (Figure S3) was extracted from several independent images, showing a particle size variation from 80 to 360 nm. As already seen in the XRD patterns the synthesized particles are highly crystalline (Figure S2c). The crystal lattice is homogeneous until the surface of the NP, and a lattice spacing of 2.85 Å can be observed corresponding to the $d_{2|2|0}$ spacing of Co_3O_4, which indirectly confirms that the surface of the cubic NPs is (1|0|0) terminated.

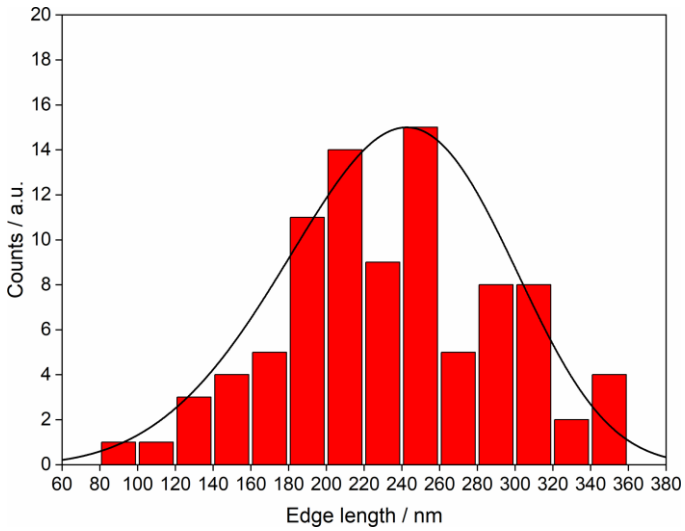

Figure S3. Size distribution with Weibull function of cubic Co_3O_4 nanoparticles (total number of measured particles: 100).

The Co 2p XPS spectrum (Fig. S4a) shows the typical pattern for Co_3O_4 with an asymmetric peak in the Co $2p_{3/2}$ region due to the presence of Co^{3+}, which is located at 779.6 eV.[4] The formation of phase impurities such as CoO and $Co(OH)_2$ can be excluded.[5] In the O 1s spectrum (Fig. S4b) a pronounced peak at ca. 529 eV indicates the lattice oxygen in Co_3O_4. In contrast, the second peak at 532 eV shows the presence of hydroxides or oxyhydroxides on the particle surface due to surface oxidation.[6] In addition, the peak at 533 eV at the characteristic binding energy for C-O bonds indicates adsorbed carbonate species.

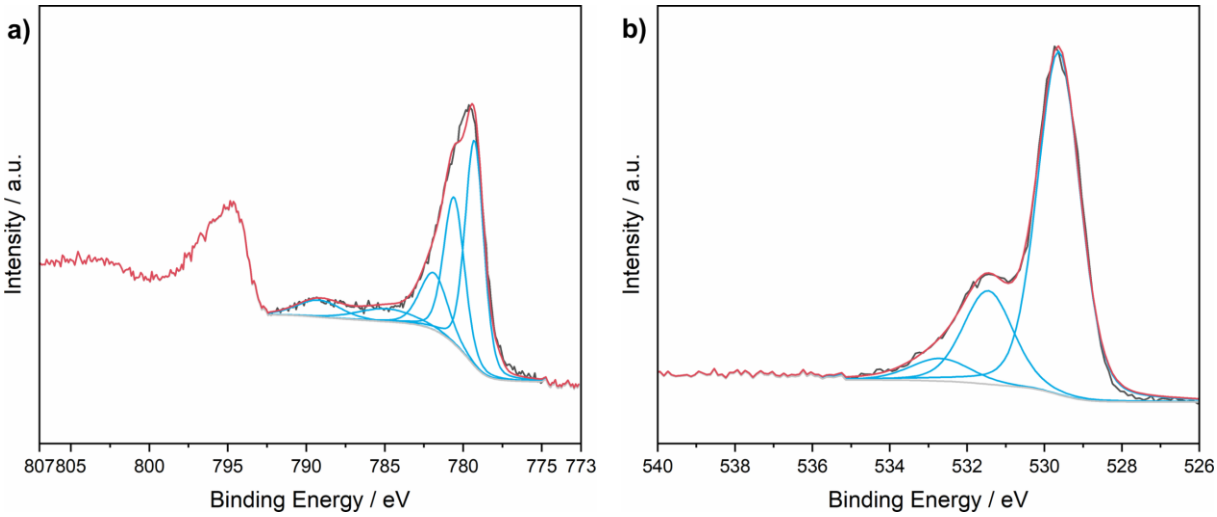

Figure S4. a) Co 2p and b) O 1s XPS spectra of Co_3O_4 cubes.

The FT-IR spectrum (Fig. S5) shows the characteristic pattern for spinel-type materials with the octahedral Co^{3+}-O vibration at 550 cm^{-1} and the tetrahedral Co^{2+}-O mode at 665 cm-1.[7] The two weaker bands at 1426 and 2913 cm^{-1} might indicate carbonates on the particle surface and O-H stretching vibrations from adsorbed water.[8]

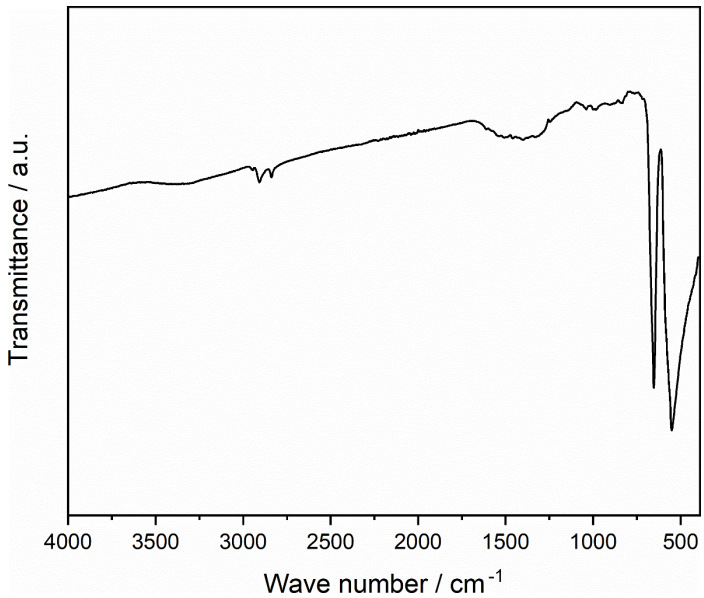

Figure S5. FT-IR spectra of cubic Co_3O_4 nanoparticles.

Section 3: SECCM experiments and electrochemical data evaluation

Sample preparation:

A glassy carbon plate was polished with a diamond suspension using particle sizes in descending order (1 µm, 0.3 µm, 0.05 µm). The plate was polished for 3-4 min with each particle size. After the plate was cleaned with ethanol and water, SEM was used to confirm that surface contamination from the polishing process could be entirely removed. The Co_3O_4 nanocubes were dispersed in a solution of toluene containing oleylamine. This mixture is then tip sonicated for 15 min with 40% amplitude control to gain a good separation of the nanoparticles, which is highly important for the SECCM measurement (Figure S7). This well-dispersed solution is then drop-cast onto the cleaned glassy carbon plate and dried under air for 15 min. The glassy carbon plate is heated at 200 °C in air to remove the oleylamine from the surface of the nanoparticles.

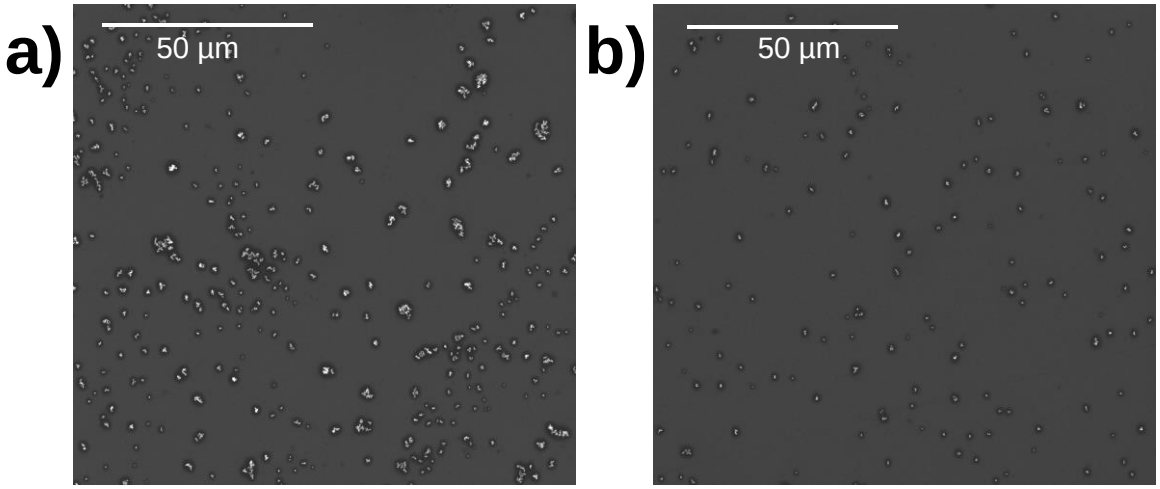

Figure S6. a) Particle separation without using the tip sonication (scale: 50 µm), and b) particle separation with tip sonication (scale: 50 µm)

Capillary preparation:

A quartz capillary is pulled using a laser puller (P-2000, Sutter Instruments) to obtain nanopipettes used in SECCM experiments. A one-line program was used with the following parameters: Heat 730-780, Filament 3, Velocity 30, Delay 130, Pull 80-100. The so obtained capillaries possessed a diameter of 400 nm – 500 nm, as shown in Figure S8. A platinum wire with a diameter 0.25 mm was used as quasi-reference/counter electrode. This wire was flame heated prior to the insertion into the capillary from the back, then dipped in aqua regia for 4-5 s and washed with distilled water to remove possible impurities. The capillary was then filled with a solution containing 0.1 mM [(Os (2, 2'-bipyridine)$_2$(N, N'-dimethyl-2, 2´-biimidazole)] $(PF_6)_3$ in 50 mM KOH using a MicroFil needle with 0.1 mm inner diameter (MF34G-5, World Precision Instruments).

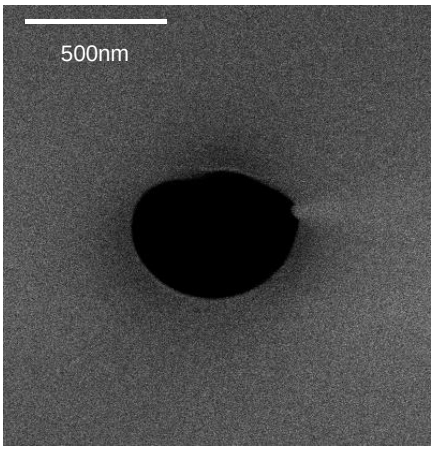

Figure S7. SEM micrograph of one of the capillary opening

SUPPORTING INFORMATION

SECCM experiment

Positioning: The filled capillary is placed close to the surface of the sample with the help of an optical microscope (Figure S9a). Once the coarse positioning of the capillary is done, the sample is moved closer to the capillary meniscus at the speed of 1-2 µm/s with the help of a piezo nanocube.

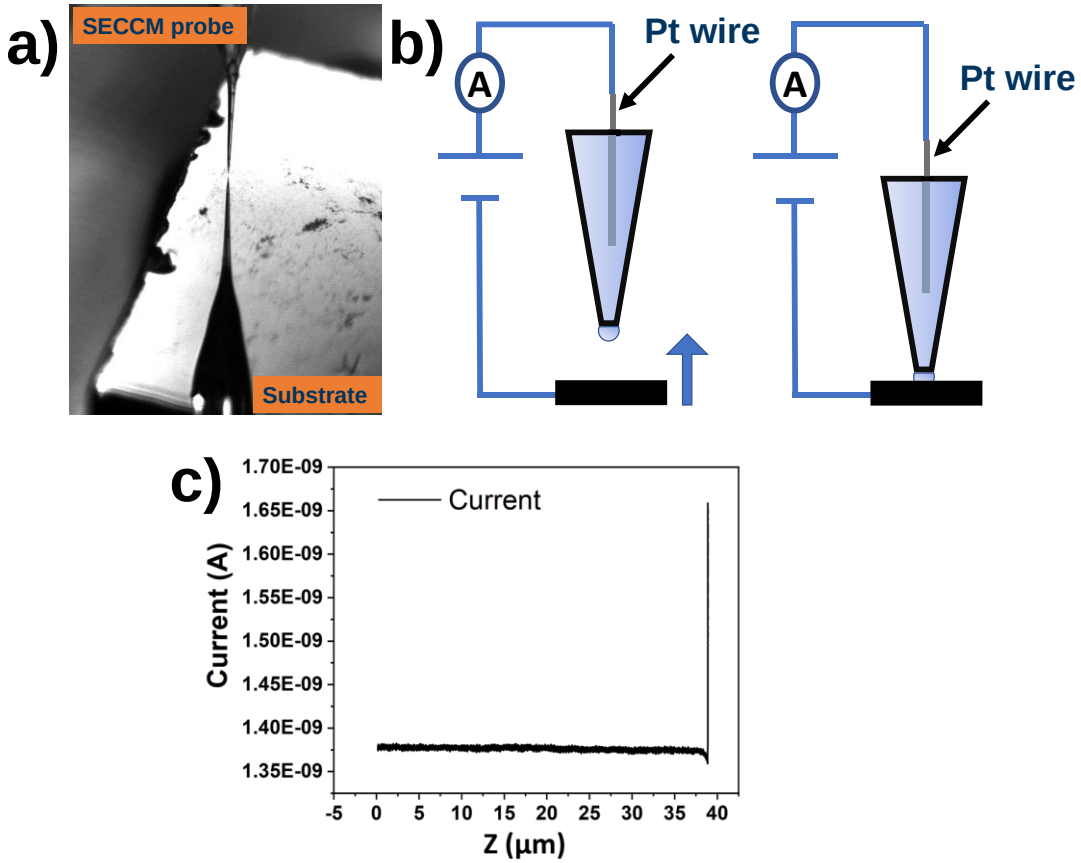

Figure S8. (a) Coarse positioning of the capillary above the sample surface. (b) Fine positioning with current feedback function (c) Approach curve obtain from fine positioning

Approach: For the final approach a current feedback threshold of 2-3 pA higher than the noise level was used to stop the approach of the sample towards the capillary. As soon as the meniscus of the nanodroplet at the lower orifice of the SECCM capillary touches the sample surface, a sharp spike in the current response is observed, and the approach is automatically stopped (Figure S9c).
SECCM measurement: Once the first approach was successfully performed, the scan was initiated in a 100 µm x 100 µm area using the hopping mode. Four cyclic voltammograms in the potential window from 0 to 0.6 V vs the Pt wire quasi reference electrode with scan rates of 0.1 V/s, 0.25 V/s, 0.5 V/s, 1 V/s and one linear sweep voltammogram in the potential window of 0 to 0.92 V vs Pt wire with the scan rate of 1 V/s were recorded from each landing point. Once the measurement at one spot was completed, the capillary was retracted by 6 µm with a velocity of 5 µm/s and subsequently moved laterally by 10 µm to the next spot of the scan with a lateral speed of 10 µm/s resulting in 100 measuring spots within the scanned area.

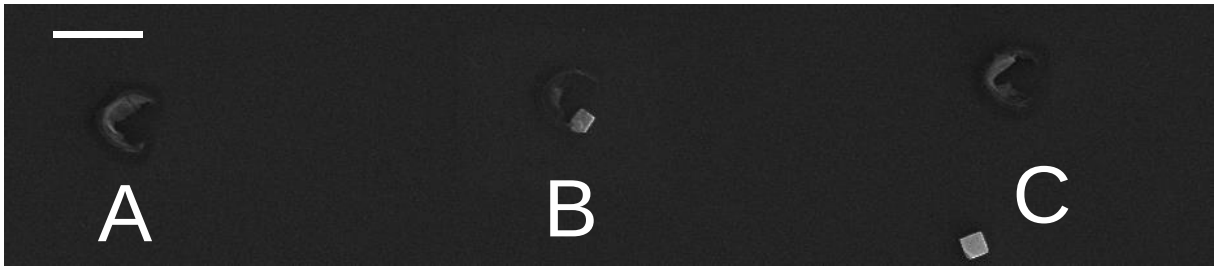

Figure S9. SEM micrographs of landing spots on particles (B) along with nearby landing spots on glassy carbon (A and C). (Scale bar: 1 µm)

SUPPORTING INFORMATION

Data processing and analysis:

The ASCII files are extracted from tdms file format for each spot using a specifically programmed conversion software. These raw data files are processed with Matlab R2020a and then plotted in Origin for further analysis.

a) Potential conversion to RHE:
The redox potential of the Os complex is 1.35 V vs RHE as reported earlier.[1] The $E_{1/2}$ value calculated from cyclic voltammogram of adjacent carbon landing spot were subtracted from the redox potential of the Os complex, and that value was added to the potential values from the voltammograms vs the Pt quasi-reference electrode to convert them to the RHE scale.

b) Carbon current correction:

$$I_{corrected} = I_{original} - I_{average\ of\ nearby\ carbon\ spot}$$

The current response of nearby landing spots on the glassy carbon plate (for example figure S10 spot A and C) is averaged and then used to correct the obtained current response at spot B by the bare carbon current response.

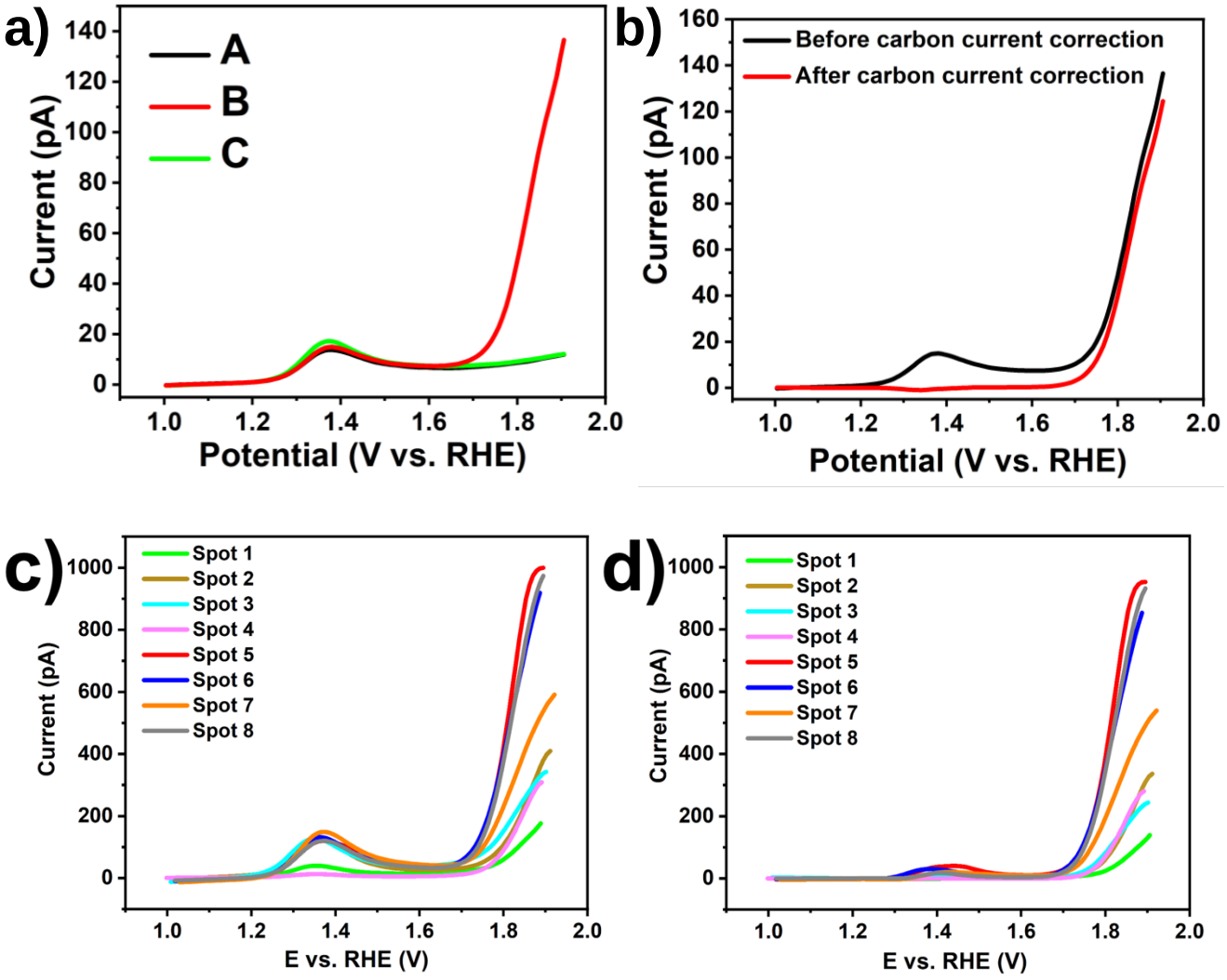

Figure S10. a) Linear sweep voltammograms of spots shown in figure S9. b) Linear sweep voltammogram before and after carbon current correction. Linear sweep voltammograms of spots shown in figure 1 where c) is before and d) after the carbon current correction.

c) TOF calculation:

$$TOF = \frac{i \times S}{4 \times n \times F}$$

where i is the current density at a specific applied potential, S is the electrochemical surface area, 4 is number of transferred electrons during the OER, n is the number of moles of exposed cobalt atoms present at surface of the NP, F is the Faraday constant.

Calculation of the number of Co atoms at the surface of the nanoparticles:

The atom density at the exposed surface planes is calculated using the crystallographic software VESTA for counting the Co atoms present at the exposed 1|0|0 surface plane of the Co_3O_4 nanocube. The number of exposed Co atoms at the 1|0|0 facet is determined to be two. The atoms at the four edges of the plane are shared by four adjacent planes, whereas an atom at the centre of the plane is considered as a full atom. Via the known unit cell constant a, the area A of the (1|0|0) plane and with this the atom density per m^2 can be calculated.

Total number of Co atoms: 4 x ¼ + 1 x 1 = 2

Surface area 1|0|0 plane: $A_{plane} = a^2 = (8.065\ Å)^2 = 6.5044 \cdot 10^{-19}\ m^2$

Atom density: $N/A = 2/6.5044 \cdot 10^{-19}\ m^2 = 3.07483 \cdot 10^{18}$ Co atoms / m^2

Geometric surface area cubic NP: $A_{NP} = 5 \times a^2$ (a = edge length of the NP)

The contact area is not considered as electrochemical active surface area.

n = mol surface Co atoms = $\frac{atom\ denisty\ 1|0|0 \times surface\ area\ cubic\ nanoparticle}{N_A}$

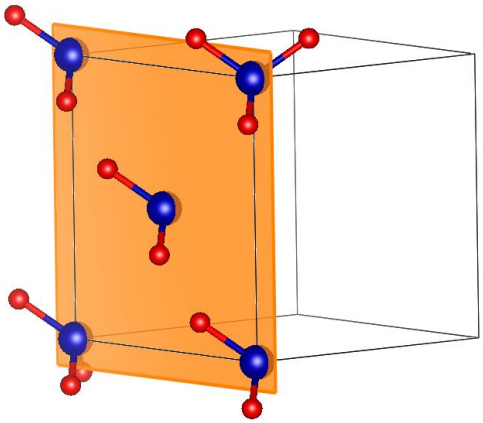

Figure S11. Illustration of surface atoms present in (1|0|0) plane of the Co_3O_4 cube

Relation of TOF values with edge length of particles:

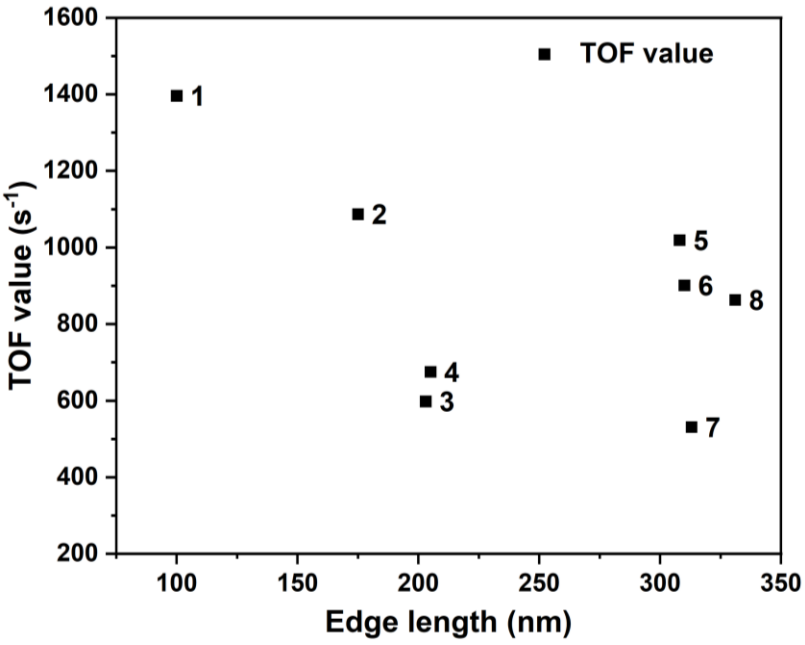

Figure S12. Plot of TOF values against edge length of particles for the measuring sites as shown in figure 1.

SUPPORTING INFORMATION

Section 4: Particle at the tip

CNE fabrication and FIB processing of the obtained CNEs:

Quartz capillaries were pulled using a P-2000 laser puller (Sutter Instruments) using the following pulling parameters: HEAT=740, FILAMENT=4, VELOCITY=45, DELAY=130, and PULL=100. The resulting quartz glass capillaries were filled with carbon employing a fully automatised set-up.[9] In this set-up a propane (Air Liquide, technical grade)/butane (Air Liquide, 99.5%) gas mixture is decomposed under a protective argon counter-flow (Air liquid, 99,999%). A two-step pyrolysis protocol is applied, in which in a first step a temperature of 980°C ± 5°C is applied to form a highly conductive carbon film through the whole capillary. In a second step, a temperature of 800 °C ± 5 °C is applied followed by a cool down phase of 35 s to a temperature of around 475 °C.

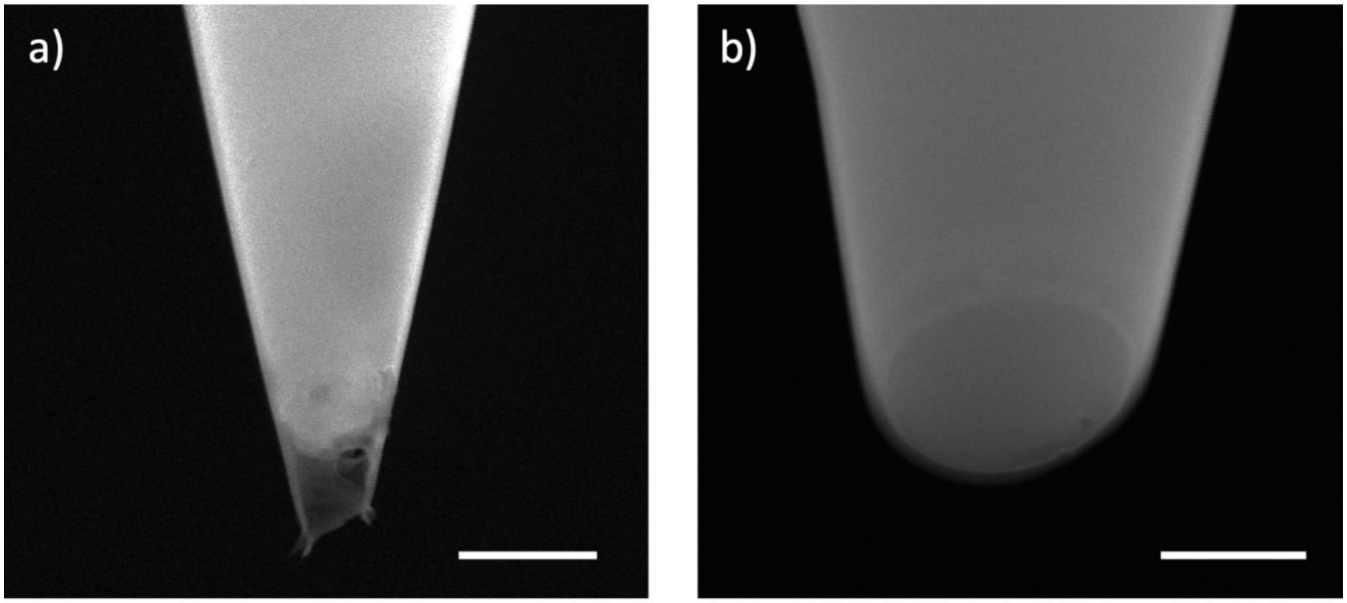

Figure S13. SEM micrographs of a) a CNE as prepared and b) a disc-shaped CNE after FIB processing. Scale bar is equal to 500 nm

In Figure S13a an as-prepared CNE is shown, which is not offering the planar surface for the particle placement. The transparent part of the tip of the CNE is the bare quartz glass capillary which was not filled with carbon. The carbon is showing a recession of roughly 300 nm. Hence, FIB milling is performed in the SECM using Ga ions to cut the electrode at a diameter of 500 to 600 nm, resulting in a perfectly disc-shaped CNE (Figure S13b). A FIB current of 100 pA with an acceleration voltage of 30 kV was applied for about 1 min until the electrode is cut.

Surface modification of the CNE:

The modification of the carbon surface of the CNE is highly important to obtain an improved interaction between the particle and the CNE. Without the surface modification, the probability that the nanoassembly is still intact after the heat treatment is very low. For the surface modification, the protocol from our previously reported study was adapted.[10] An ethanol solution containing 3.3 mM N-Boc-ethylenediamine and 0.1 M $LiClO_4$ was used. The CNEs are then electrochemically modified by applying a single 20 ms oxidative pulse at 1.5 V vs. Ag/AgCl/3 M KCl. During this potential pulse, the non-protected amino group N-Boc-ethylenediamine is oxidatively grafted to the carbon surface, but importantly the layer is not blocking the electron transfer. After the oxidative pulse, the electrodes were washed in ethanol absolute to remove any excess of N-Boc-ethylenediamine, followed by the acidic cleavage of the BOC protection group in 4 M H_2SO_4. The resulting amino-group modified CNE surface is washed by dipping it into ethanol to remove excess H_2SO_4.

Baseline current subtraction for comparison with the SECCM data:

Due to the measurement conditions as used in the SECCM measurments, namely 0.05 M KOH solution is 0.1 mM of the Os-complex, the oxidation of the Os complex is leading to a sigmoidal voltammogram at the nanoelectrode and is hence reaching a steady-state current at higher potentials of about 1.4 V vs. RHE (Figure S14a). Since the electrochemical active surface area of the CNE (600 nm diameter) is increased by around 60% when a single cubic Co_3O_4 particle (edge length 300 nm) is attached to it, a subtraction of just a bare carbon electrode response from the one measured with a particle attached to its surface is not possible. However, the steady-

state current of the Os complex oxidation can be subtracted in the potential range of the OER. Moreover, if one is comparing the measured current in Figure S14a with the one in Figure S14b it is clear that the steady-state current of the Os-complex is tiny. Nevertheless, subtraction of the steady-state current as shown in Figure S14c was performed at 1.6 V vs RHE, causing the slight offset to negative values at lower potentials. By this, it can be ensured that no current which is due to the Os-complex oxidation is contributing to the OER current and wrongly impacting TOF calculations.

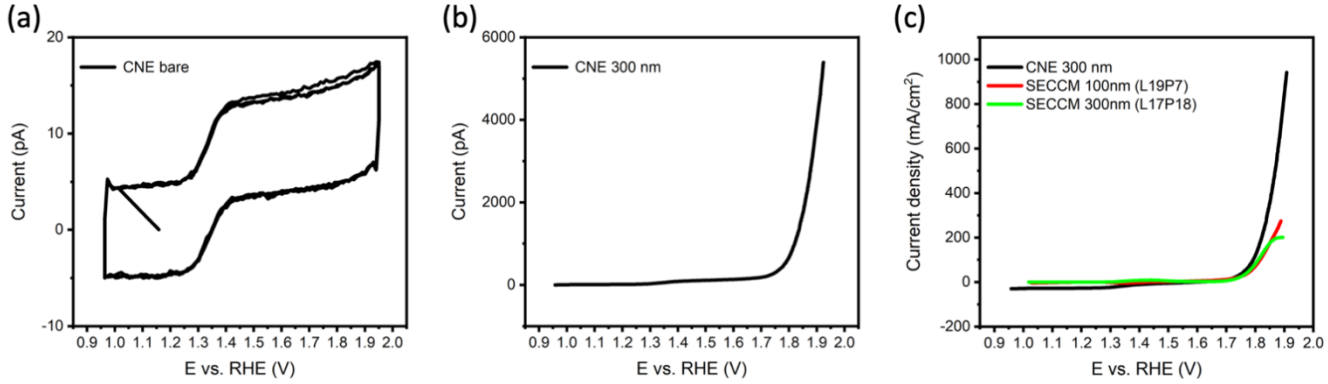

Figure S14. a) CV of a bare CNE; b) LSV of a Co_3O_4@CNE nanoassembly with a nanocube with an edge length of 300 nm; and c) LSV from b) normalised with respect to the geometric surface area of the cube and Os-complex oxidation current corrected. All measurements were performed in 0.05 M KOH containing 0.1 mM Os-complex with a scan rate of 1 V s^{-1}

TEM holder for investigating CNE in the TEM:

For investigating the CNEs by means of identical-location TEM, a new TEM holder was designed to achieve easier handling of the CNE (Figure S15). Using the newly designed TEM holder, the CNEs can be inserted inside the TEM without cutting the CNE to a specific length. The hole which was drilled inside the TEM holder is deep enough to handle an electrode length of up to 6 cm. Additionally, the TEM holder can perform a high angle α-tilt as the holder has the same geometry of the commercial tomographic holder with ± 82 ° tilt angle. The holder can therefore investigates the CNE-attached nanoparticle at specific angles.

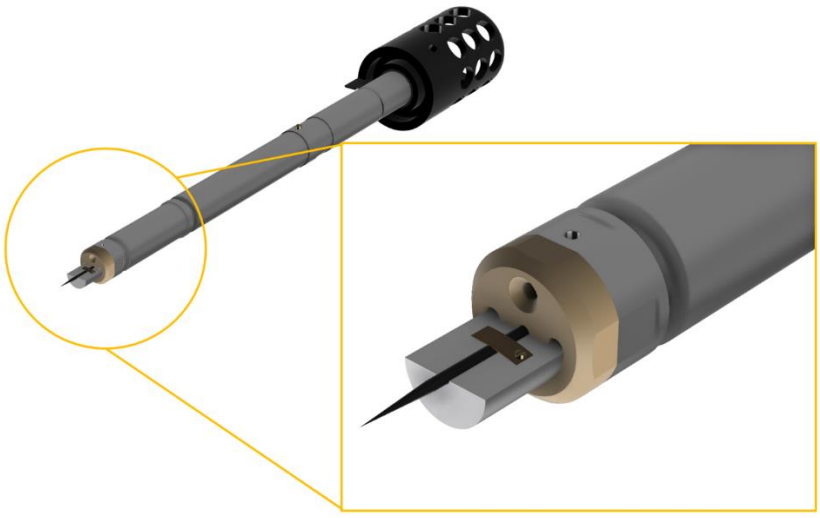

Figure S15. Illustration of the newly designed TEM holder for the investigation of particle-modified CNEs.

Section 5: HR-TEM of Co_3O_4 cubes at low concentration electrolyte

The crystal lattice with a spacing of 2.04 Å corresponding to the $d_{4|0|0}$ of Co_3O_4 (2.01 Å) of the measured Co_3O_4 cube (Figure S16a) is homogeneously spread over the entire nanocube surface. After the electrochemical measurement, no significant changes in the surface structure of the particle is visible. The visible lattice fringes are reaching the particle surface (Figure S16b) with a spacing of 2.05 Å corresponding to the $d_{4|0|0}$ of Co_3O_4 (2.01 Å). An additional spacing of 2.88 Å is observed corresponding to the $d_{2|2|0}$ of Co_3O_4 (2.85 Å). This demonstrates that at electrolyte concentrations of 0.05 M KOH as used for the SECCM measurements, the imposed electrochemical challenges are not sufficient to impose structural changes of the nanocube. This is attributed to the high voltammetric scan rate and the low alkalinity leading to a comparatively low electrochemical stress.

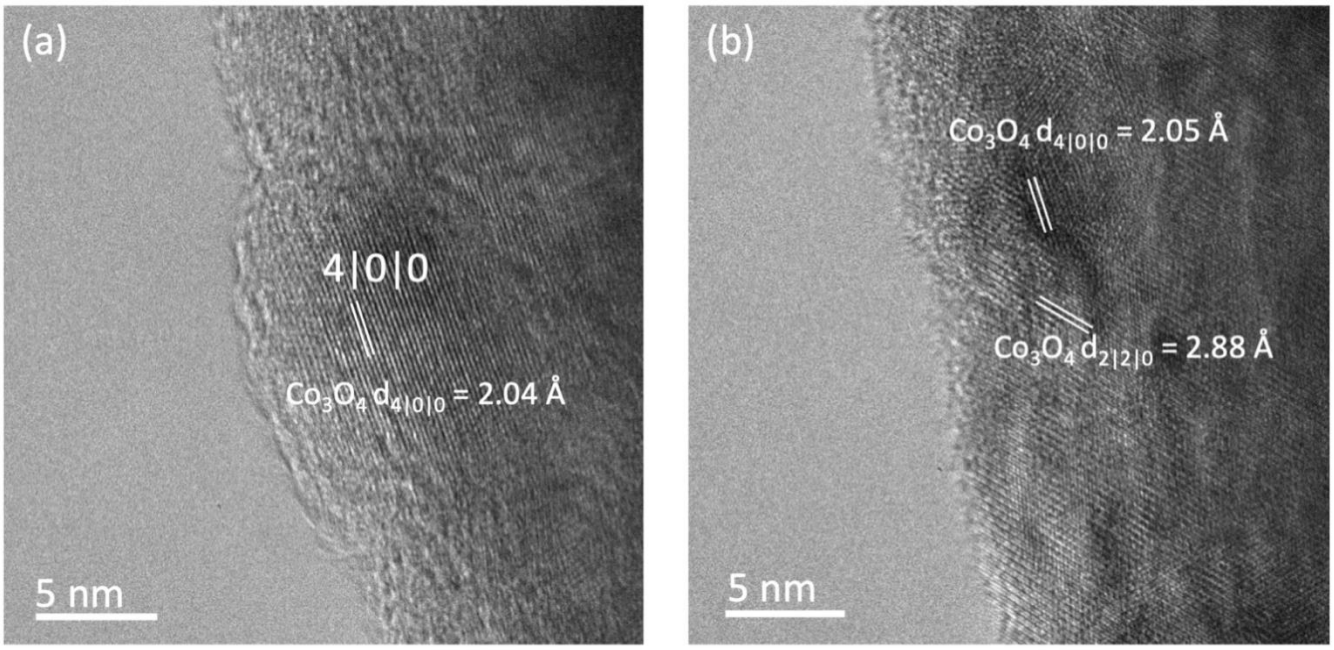

Figure S16. HR-TEM micrographs of the Co_3O_4@CNE nanoassembly investigated in Figure S14 before a) and after b) the electrochemical measurement.

References

[1] T. Tarnev, H. B. Aiyappa, A. Botz, T. Erichsen, A. Ernst, C. Andronescu, W. Schuhmann, *Angew. Chem. Int. Ed.* **2019**, *58*, 14265; *Angew. Chem.* **2019**, 131, 14403

[2] N. Ebejer, A. G. Güell, S. C. S. Lai, K. McKelvey, M. E. Snowden, P. R. Unwin, *Annu. rev. Anal. Chem.* **2013**, *6*, 329.

[3] J. P. Picard, G. Baud, J. P. Besse, R. Chevalier, *J. Less-Common Met.* **1980**, *75*, 99.

[4] B. Qiu, W. Guo, Z. Liang, W. Xia, S. Gao, Q. Wang, X. Yu, R. Zhao, R. Zou, *RSC Adv.* **2017**, *7*, 13340.

[5] a) M. C. Biesinger, B. P. Payne, A. P. Grosvenor, L. W. Lau, A. R. Gerson, R. S. Smart, *Appl. Surf. Sci.* **2011**, 2717; b) L. Lukashuk, N. Yigit, H. Li, J. Bernardi, K. Föttinger, G. Rupprechter, *Catal. Today* **2019**, *336*, 139.

[6] R. Zou, K. Xu, T. Wang, G. He, Q. Liu, X. Liu, Z. Zhang, J. Hu, *J. Mater. Chem. A* **2013**, *1*, 8560.

[7] H. Xu, Z. Hai, J. Diwu, Q. Zhang, L. Gao, D. Cui, J. Zang, J. Liu, C. Xue, *J. Nanomater.* **2015**, *2015*, 1.

[8] a) D. Klissurski, E. Uzunova, *Chem. Mater.* **1991**, *3*, 1060; b) E. U. Ikhuoria, S. O. Omorogbe, B. T. Sone, M. Maaza, *Sci. Technol. Materials* **2018**, *30*, 92.

[9] P. Wilde, T. Quast, H. B. Aiyappa, Y.-T. Chen, A. Botz, T. Tarnev, M. Marquitan, S. Feldhege, A. Lindner, C. Andronescu, W. Schuhmann, *ChemElectroChem* **2018**, *5*, 3083.

[10] T. Quast, H. B. Aiyappa, S. Saddeler, P. Wilde, Y.-T. Chen, S. Schulz, W. Schuhmann, *Angew. Chem., Int. Ed.* **2021**, *60*, 3576; *Angew. Chem.* **2021**, 133, 3619.

Author contributions

T. Quast: Data collection (equal), data interpretation (equal), writing of initial draft (lead)
S. Varhade: Data collection (equal), data interpretation (equal), writing of initial draft (supporting)
S. Saddeler: Data collection (supporting), data interpretation (supporting)
Y.-T. Chen: Data collection (supporting), data interpretation (supporting)
C. Andronescu: Administration (equal), funding acquisition (equal), data interpretation (equal)
S. Schulz: Project administration (equal), funding acquisition (equal), data interpretation (equal)
W. Schuhmann: Research idea and concept (lead), project administration (equal), funding acquisition (equal), data interpretation (equal), writing of manuscript (supporting)